Substrate engineering for high quality emission of free and localized excitons from atomic monolayers in hybrid architectures

OLIVER IFF[1,+], YU-MING HE[1,+], NILS LUNDT[1], SEBASTIAN STOLL[1], VASILIJ BAUMANN[1], SVEN HÖFLING[1,2], AND CHRISTIAN SCHNEIDER[1,*]

[1] Technische Physik and Wilhelm Conrad Röntgen Research Center for Complex Material Systems, Physikalisches Institut, Universität Würzburg, Am Hubland, D-97074 Würzburg, Germany
[2] SUPA, School of Physics and Astronomy, University of St Andrews, St Andrews, KY16 9SS, United Kingdom
[+] These authors contributed equally
[*] Corresponding author: christian.schneider@physik.uni-wuerzburg.de

Compiled March 31, 2017

Atomic monolayers represent a novel class of materials to study localized and free excitons in two dimensions and to engineer optoelectronic devices based on their significant optical response. Here, we investigate the role of the substrate on the photoluminescense response of $MoSe_2$ and WSe_2 monolayers exfoliated either on SiO_2 or epitaxially grown InGaP substrates. In the case of $MoSe_2$, we observe a significant qualitative modification of the emission spectrum, which is widely dominated by the trion resonance on InGaP substrates. However, the effects of inhomogeneous broadening of the emission features are strongly reduced. Even more strikingly, in sheets of WSe_2, we could routinely observe emission lines from localized excitons with linewidths down to the resolution limit of 70 μeV. This is in stark contrast to reference samples featuring WSe_2 monolayers on SiO_2 surfaces, where the emission spectra from localized defects are widely dominated by spectral diffusion and blinking behaviour. Our experiment outlines the enormous potential of III-V-monolayer hybrid architectures to obtain high quality emission signals from atomic monolayers, which are straight forward to integrate into nanophotonic and integrated optoelectronic devices.

OCIS codes: *(250.5230) Photoluminescence; (300.6280) Spectroscopy, fluorescence and luminescence; (270.0270) Quantum optics; (300.6470) Spectroscopy, semiconductors*

http://dx.doi.org/10.1364/optica.XX.XXXXXX

1. INTRODUCTION

Monolayers of transition metal dichalcogenides have moved into the focus of solid state spectroscopy, since these new materials feature a variety of unique optical properties. Monolayers composed of the transition metal Mo or W and the chalcogene Se, S and Te crystallize in a honeycomb lattice which lacks an inversion center. This yields a characteristic bandstructure, where the direct bandgap transitions are located at the K and K′ points of the hexagonal Brillouine zone. Due to the missing inversion symmetry these points are inequivalent and are occupied by charges of opposite spin. This leads to coupling of the spin and the according K valley, introducing a new degree of freedom which is accessible via optical selection rules. As a result each valley can be distinctly addressed by the polarization of an injection laser, which leads to novel spinor effects in these systems [1–6]. In addition, so called valley excitons are formed, which feature an extraordinarily high binding energy exceeding 300 meV [7]. This is a consequence of reduced dimensions, reduced dielectric screening and flat bands leading to a heavy exciton mass. In most of these materials, even up to ambient conditions, the absorption and luminescence spectrum is dominated by excitonic effects, rather than by direct interband transitions. While the general properties, such as the exciton frequency, and the trion binding energy are primarily determined by the monolayer itself, the surrounding environment still has a major influence on the optical properties. For instance, it has been shown that excitons in monolayers of MoS_2 sensibly react on absorbed molecules on the surface [8], and energy shifts resulting from capping have been reported [9]. Similarly, the choice of the substrate can have a significant effect on the luminescence properties of the free monolayer excitons, as well as the emission features from localized excitons which were recently identified as novel sources of single photon streams [10–14]. Furthermore, these kind of quantum emitters have been observed in monolayers laying on top of

patterned arrays of nano pillars [15, 16]. Here, we study the excitonic properties of exfoliated monolayers of $MoSe_2$ and WSe_2 at cryogenic temperatures, which were transferred onto SiO_2/Si as well as InGaP/GaAs heterostructures. For the case of $MoSe_2$, we observe a strong reduction of the inhomogeneous broadening of the dominant trion feature as epitaxial substrates are utilized. In monolayers of WSe_2, we focus on the emission of localized excitons. This quantum dot like features are strongly broadened and disturbed by their environment on the insulating glass substrates. In stark contrast, the semiconducting InGaP/GaAs substrates have a suitable band-alignment with respect to $MoSe_2$ and WSe_2 (compared to GaAs) and less heavy surface oxidation (compared to AlGaAs), facilitating dramatically reduced charge fluctuations and yielding stable and robust emitters of single photons on an epitaxial platform. Furthermore, InGaP is a well-established material platform for integrated photonic devices, such that our work can easily be extended to utilize monolayer materials in more complex, integrated schemes.

2. SAMPLE STRUCTURE AND SETUP

The investigated monolayers were produced by mechanical exfoliation from a $MoSe_2$ or a WSe_2 bulk crystal with scotch tape. After confirming their monolayer nature via their distinct photoluminescence and the color contrast in an optical microscope, they have been transferred onto the designated target substrate via a dry-stamp method [17]. Using this technique, flake sizes of around 30 μm * 50 μm have been fabricated. Two different sample types have been implemented which are sketched in fig. 1 (a). The monolayers were transferred onto substrates composed of a 90 nm SiO_2 layer ontop of a Si substrate. The other substrate is made of a 250 nm thick $In_{0.49}Ga_{0.51}P$ layer which has been grown lattice-matched onto a semi-insulating GaAs by means of gas-source molecular beam epitaxy.

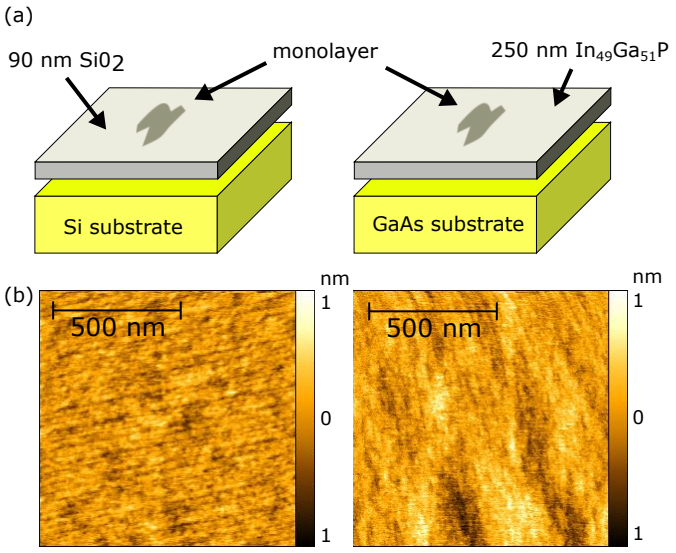

Fig. 1. (a) Schematic drawing of the investigated heterostructures: 90 nm SiO_2 on a Si substrate, and 250 nm $In_{0.49}Ga_{0.51}P$ lattice matched to a GaAs substrate. The monolayers were transfered onto each substrate, using the dry-stamp technique. (b) AFM measurements of the used samples. SiO_2 has a root-mean-squared roughness of 0.15 nm, while $In_{0.49}Ga_{0.51}P$ has 0.29 nm.

In order to get an impression of the samples' surface quality we performed atomic force microscope (AFM) measurements, which can be seen in fig. 1 (b). The root-mean-squared roughness of both samples is of the same magnitude. Specifically, the SiO_2 surface characterized by a roughness of ≈ 0.15 nm, while the InGaP surface features a comparable value of 0.29 nm. Optical characterization was carried out in a standard microphotoluminescence setup (μPL). The samples were attached to the cold-finger of a liquid helium flow cryostat and the luminescence from the flake was collected by a 50x objective (NA=0.42) in a confocal microscope system. The structures were excited by a continuous-wave(cw) 532 nm laser. Photoluminescence measurements were performed using a Princeton-Instrument SP2750i spectrometer equipped with a liquid nitrogen cooled charge coupled detector and a 1500 $\frac{\text{lines}}{\text{mm}}$ grating ($\Delta E_{\text{Res}} \approx 70$ μeV) for the high resolution images or a 300 $\frac{\text{lines}}{\text{mm}}$ grating for overview spectra. The PL could also be collected into a fiber coupled Hanbury Brown and Twiss setup (HBT) with a timing resolution of approximately 570 ps to measure the second order field correlation of the emission, after passing through a pair of band-pass filters (1 nm bandwidth).

3. EXPERIMENTAL RESULTS AND DISCUSSION

First, we investigate the impact of the two aforementioned substrates on the emission characteristics of $MoSe_2$ monolayers. Fig. 2 depicts a series of photoluminescence spectra of the Si/SiO_2-$MoSe_2$ structure which were recorded subsequently under nominally the same conditions and without blanking the laser. The spectra were taken in a time span of 10 minutes at a constant laser power of 50 μW. We observe the common spectral signatures of $MoSe_2$ monolayers: At 1.657 eV, the free exciton (X) is clearly visible. On the low energy side, the negatively charged trion (X-) emerges at 1.625 meV, yielding a trion binding energy of 32 meV. Noteworthily, during the series, the initial exciton intensity decreases and the trion intensity increases until both signals converge to a constant intensity ratio $I_{X-}/I_X \approx 2$ after roughly 5 minutes. This behaviour can be explained by a photo induced doping effect which introduces new free carriers into the system, enhancing the formation of trions [18, 19] at the expense of free neutral excitons. At all accessible pump powers, we observed emission from both the X as well as the X- resonance in this case. A significantly more in depth analysis of the interplay between excitons and trions in $MoSe_2$ on insulating substrates can be found in [20]. On the contrary, on

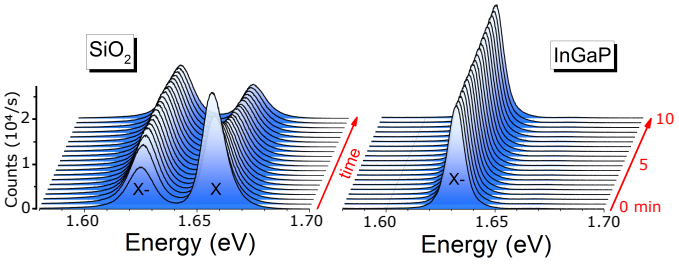

Fig. 2. Monolayer photoluminescence at 50 μW, recorded over ten minutes. For $MoSe_2$ on SiO_2, the exciton intensity diminishes over time while the trion grows in intensity. For the $MoSe_2$-InGaP heterostructure , the trion dominates the spectrum by a large margin.

the GaAs/InGaP-$MoSe_2$ heterostructures, the free exciton is not visible at 50 μW laser power while only the trion-attributed resonance can be clearly observed with an energy of 1.632 eV. At high pump power we see a strongly suppressed signal from the exciton at around 1.665 eV, being about two orders of magnitude weaker in intensity than the trion. The spectral energy shift of approx 7meV compared to the SiO_2-$MoSe_2$ stack occurs reproducibly in different flakes, and is most likely a consequence of the modified dielectric environment. Remarkably, the overall intensity of this trion resonance does not change with time, indicating that the system natively has access to a great amount of free carriers. We note, that both monolayers originate from the same bulk crystal and therefore we can rule out inherent doping of the flake itself as a reason of this behaviour. In fig. 3 we depict the result of a power series from both samples. The non-resonant excitation power was ramped from 50 μW up to 6 mW, and we plot the trions' integrated intensity and linewidth. By taking into account realistic parameters (absorption coefficient $\approx 4.0 * 10^5$ [21], lifetime $\approx$ 1 ps lifetime [22]), we estimate an upper bound of the exciton density on the order of $2 * 10^9 cm^{-2}$ in this experiment. With increasing power, the intensity of the observed resonances rises approximately linearly as shown in fig. 3(a). Fitting the data (red lines) to a straight line gives a slope of 0.96 for SiO_2 respectively 0.92 for InGaP, in good agreement with the expected slope of 1 for charged excitons. At higher output power (>1 mW) the emissions start to show a saturation behaviour, independent from the used substrate caused by exciton annihilation [23]. Another important parameter is the corresponding full width at half maximum (FWHM) of the studied signal, which is plotted in fig. 3 (b). On the glass substrate the linewidth of the trion reaches a value around 13 meV for small laser power. Increasing the power yields a progressive broadening of the emission line, reaching approximately 16 meV at 6 mW pump power. We assume, that this power induced broadening of the trion resonance is a consequence of local heating from the pump laser, but it could be also induced by additional charges which accumulate in the monolayer and at random positions at the heterointerface [19]. This charge puddling effect is known to occur on SiO_2 surfaces [24], which induce a randomly varying inhomogeneity on the photoluminescence response. Contrary to this, the linewidth on the InGaP sample is as small as 6.5 meV, surpassing its SiO_2 counter part by

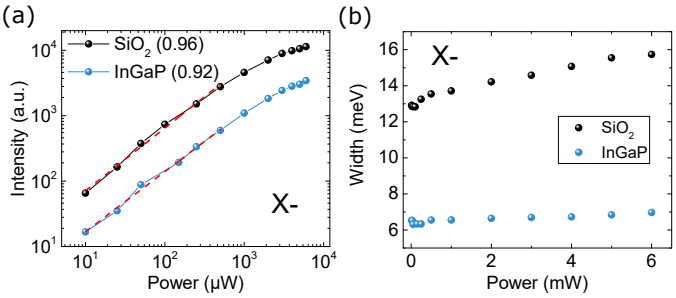

Fig. 3. (a) Input-output characteristics of the trion intensity for $MoSe_2$ on SiO_2 and $MoSe_2$ on InGaP samples with an almost linear slope of 1. Dashed red lines are fitting curves. (b) Corresponding FWHM of the trion. On SiO_2, it starts at 13 meV, increasing at higher powers up to 16 meV. On InGaP, the linewdith is 6.5 meV, which stays almost constant with regard to laser output.

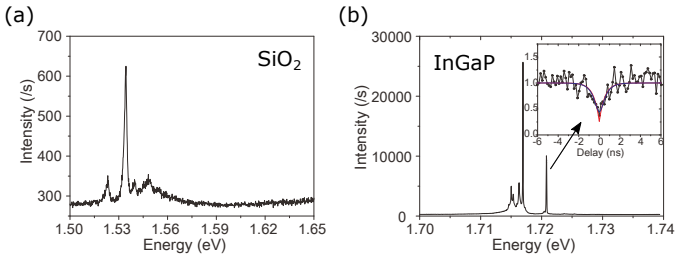

Fig. 4. (a) The typical PL spectrum of the localized exciton in the monolayer WSe_2 exfoliated onto a SiO_2/Si substrate, measured at a sample temperature of nominally 4.5 K. (b) PL spectrum of the localized exciton in the monolayer WSe_2 with the InGaP/GaAs substrate under 4.5 K. The peak energies range from 1.5 eV to 1.73 eV. The inset is the auto-correlation measurement of marked peak under a 70 nW CW laser excitation at 532 nm. The blue line in the inset is a fit with multiexcitonic model convolved with the response function. The red line is the deconvoluted curve, which shows $g^{(2)}(0)$=0.261±0.117.

a factor of 2. Even more remarkably, the linewidth stays nearly constant with increasing power and reaches just 7 meV at 6 mW laser output. This is due to a higher thermal conductivity of InGaP compared to SiO_2 [25] leading to lower local heating at the laser spot. This is also supported by an overall reduced spectral shift of InGaP during the power series. Overall, these results already outline the reduction of charge induced fluctuations in monolayer-InGaP devices, and illustrate the impact the right substrate can have on the excitonic properties of $MoSe_2$. While monolayers of $MoSe_2$ are specificly suitable to study effects of free excitons and trions, the observation of single photon emission from localized excitons have set monolayers of WSe_2 in the focus of solid state quantum photonics. Figure 4 shows a typical photoluminescence spectrum from such a localized exciton in a WSe_2 monolayer ontop of a SiO_2/Si substrate, which was excited by a continuous-wave(CW) 532 nm laser at an excitation power of 30 μW and a nominal sample temperature of 4.2 K. The photoluminescence spectrum consists of several sharp peaks with linewidths of 2 meV, centered at 1.52 eV. Such a spectral feature, which is red-shifted 180 meV from the WSe_2 free valley exciton(1.7eV), is comparable to previously reported localized emission signals in WSe_2 monolayers [26]. Compared to the weak, broad PL spectrum from the localized exciton in the WSe_2 monolayer exfoliated on the SiO_2/Si substrate, several bright, spectral resolution limited (70 μeV) PL peaks were observed from WSe_2 sheets transferred onto the InGaP/GaAs substrate (temperature of 4.5 K). Here, the PL excitation power for fig. 4 (b) is around 70 nW, which is almost three order of magnitude smaller than the nominal 30 μW for fig. 4 (a). Additionally, the right inset of fig. 4 (b) shows the cw-pumped autocorrelation histogram from the marked peak in fig. 4 (b). The emission is spectrally filtered by a pair of band-pass filters and then coupled into a fiber-based HBT-setup to measure the second order autocorrelation. The clear antibunching is observed around $\tau \approx 0$ ns which reaches down well below 0.5 and therefore proves the single photon emission. In order to account for the finite time resolution of our setup, we fit the measured data with a two sided exponential decay convolved with a Gaussian distribution

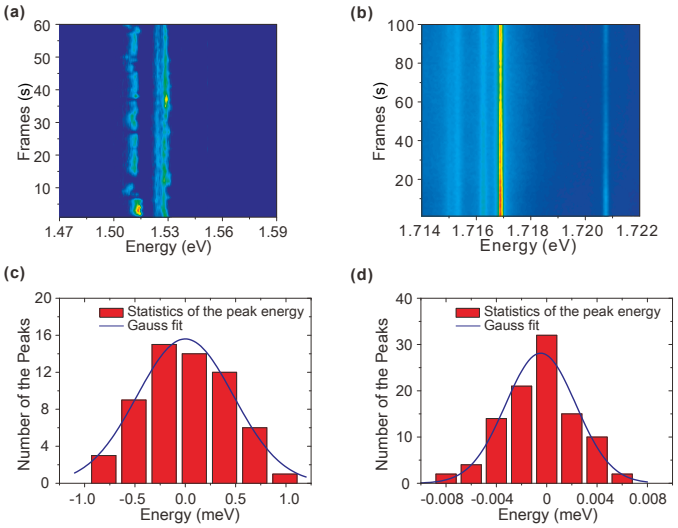

Fig. 5. (a) Spectral wandering of the localized exciton in layered WSe_2 on the SiO_2/Si substrate. (b) Emission time trace of the localized exciton in layered WSe_2 on the InGaP/GaAs substrate. Here, no obvious spectral wandering could be observed. (c) and (d) Statistics of the localized exciton peak A and peak B in Fig. 4(a) and Fig.4 (b) as a function of time. The extracted FWHM of the wandering are $(957 \pm 58)\mu$eV and $(5.583 \pm 0.582)\mu$eV respectively.

f_{Det} according to:

$$g^{(2)}_{source}(\tau) = 1 - ((1 - g^{(2)}(0)) * e^{-|\frac{\tau}{\tau_C}|}) \quad (1)$$

$$g^{(2)}_{measured}(\tau) = (g^{(2)}_{source} * f_{Det})(\tau) \quad (2)$$

Following this, we extract a deconvoluted $g^{(2)}(0)$-value of $g^{(2)}_{cw} = 0.261 \pm 0.117$.

To assess the influence of the spectral wandering on the macroscopic time scale on the emission features depicted in fig. 4 (a) and 4 (b), we record various spectra every second and combine them in the contour graph in fig. 5 (a) and 5 (b). In fig.5 (a), clear spectral wandering and jumps on the timescale of seconds are observed. Each frame is then fitted with a Lorentzian function and the statistics of the peak energies are plotted in fig. 5 (c). We find a direct contribution as large as $(957 \pm 58)\mu$eV of the long term spectral diffusion. This characteristic slow spectral jitter on such a large magnitude is commonly observed for self-assembled quantum emitters close to surfaces or interfaces which yield the capability of trapping and releasing charges. Thus, and in principle agreement with the studies presented in fig. 3 for the $MoSe_2$ case, we conclude that the spectral jumps are induced by carriers trapped via dangling bonds on the SiO_2 surface. Compared to the WSe_2 monolayer on SiO_2 substrate, no obvious spectral wandering is observed in fig. 5 (b), where the WSe_2 monolayer is transferred on the InGaP substrate. The corresponding statistics of the spectral wandering in fig. 5 (d) yields a value around 5.5μeV, which is within the linewidth fitting uncertainty. The narrowing could be attributed to fewer charge fluctuation for semiconducting environment which allows transferring trapped charges, which leads to a suppression of the long scale spectral jitter. Additionally, it has been shown that InP surfaces can be effectively passivated by S or Se, saturating many dangling bonds of the substrate [27, 28]. In this

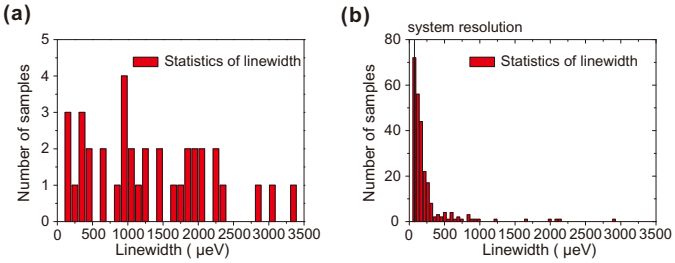

Fig. 6. (a) Statistic of the linewidth distribution for the 37 localized excitons in the WSe_2 monolayer on the SiO_2/Si substrate. The extracted minimum linewidth is 125 μeV. (b) Statistic of the linewidth distribution for the localized excitons in the WSe_2 monolayer on the InGaP/GaAs substrate. For the 72 narrowest emission lines (first bin) the average linewidth of $(74.8 \pm 12.2)\ \mu$eV is restricted by the resolution of our spectrometer (70 μeV).

scenario, one would expect to observe a more stable photon emission from the InGaP hybrid structure.

Lastly, we performed a statistical study of the influence of the different substrate on the spectral linewidth of the localized excitons in the WSe_2 monolayers. A statistical histogram for 37 randomly localized emitters from 10 different monolayers on SiO_2/Si substrate is presented in fig.6 (a). The extracted linewidths randomly fluctuate between 147 μeV to 3.3 meV. Similarly, the statistical histogram for 251 randomly localized emitters from 10 different monolayers on InGaP/GaAs is depicted in fig. 6 (b). Although linewidths of 100 μeV sharp peaks could be measured, they are not necessarily representative. Here the median linewidth of WSe_2 on InGaP (120 μeV) is close to the spectrometer resolution limit (70μeV), which is about 10 times smaller compared to the SiO_2 structure (1150 μeV). Therefore, the resolution limited, jitter free PL strongly indicates that the InGaP substrate could greatly enhance the emission properties of the localized excitons in the WSe_2 monolayer.

4. SUMMARY

In conclusion, we have studied the influence of the substrate on the emission properties of monolayers of $MoSe_2$ and WSe_2 at cryogenic temperatures. On our reference SiO_2 substrate, the luminescence of the free exciton and trion in $MoSe_2$ is notably inhomogeneously broadened, and sensitive to power broadening. The investigated localized defects occuring in WSe_2 monolayers are subject to a long term spectral diffusion induced by a slowly varying charge environment. In stark contrast, InGaP substrates show a notable effect on the charge environment, which directly leads to a reduced broadening of the trionic emission in $MoSe_2$ and in many cases eliminates the slow spectral diffusion acting on localized emission centers in WSe_2. Together with the highly developed photonic processing technology of InGaP/GaAs structures, this makes WSe_2-InGaP heterostacks very interesting for novel nanophotonic and integrated monolayer based quantum photonic architectures. Furthermore, we have observed a significantly enhanced formation of free trions in $MoSe_2$ monolayers on InGaP, which make such a platform highly suitable to study interactions of monolayer excitations with electron gases, and can likely represent a new approach towards trion polaritons in a straight forward manner and without the necessity for electrostatic gating.

ACKNOWLEDGMENTS

We acknowledge financial support by the State of Bavaria and the European Research Council (Project Unlimit-2D).

REFERENCES

1. X. Xu, W. Yao, D. Xiao and T. F. Heinz, "Spin and pseudospins in layered transition metal dichalcogenides," Nature Phys. **10**(5), 343–350 (2014).
2. A. M. Jones, H. Yu, N. J. Ghimire, S. Wu, G. Aivazian, J. S. Ross, B. Zhao, J. Yan, D. G. Mandrus, D. Xiao, W. Yao and X. Xu, "Optical generation of excitonic valley coherence in monolayer WSe_2," Nature Nanotech. **8**(9), 634–638 (2013).
3. D. Xiao, G. B. Liu, W. Feng, X. Xu, and W. Yao, "Coupled spin and valley physics in monolayers of MoS_2 and other Group-VI dichalcogenides," Phys. Rev. Lett. **108**(19), 196802 (2012).
4. K. F. Mak, K. He, J. Shan and T. F. Heinz, "Control of valley polarization in monolayer MoS_2 by optical helicity," Nature Nanotech. **7**(8), 494–498 (2012).
5. T. Cao, G. Wang, W. Han, H. Ye, C. Zhu, J. Shi, Q. Niu, P. Tan, E. Wang, B. Liu and J. Feng, "Valley-selective circular dichroism of monolayer molybdenum disulphide," Nat. Commun. **3**(6), 887 (2012).
6. H. Zeng, J. Dai, W. Yao, D. Xiao and X. Cui, "Valley polarization in MoS_2 monolayers by optical pumping," Nature Nanotech. **7**(8), 490–493 (2012).
7. A. Ramasubramaniam, "Large excitonic effects in monolayers of molybdenum and tungsten dichalcogenides," Phys. Rev. B **86**(11), 1–6 (2012).
8. J. He, K. Wu, R. Sa, Q Li, Y Wei,"Magnetic properties of nonmetal atoms absorbed MoS2 monolayers," App. Phys. Lett., **96**(8), 2014–2017 (2010).
9. D. Sercombe,S. Schwarz, O. Del Pozo-Zamudio, F. Liu, B. J. Robinson, E. Chekhovich, I. Tartakovskii, "Optical investigation of the natural electron doping in thin MoS2 films deposited on dielectric substrates," Scientific Reports, **3** 3489 (2013).
10. Y.-M. He, G. Clark, J. R. Schaibley, Y. He, M.-C. Chen, Y.-J. Wei, X. Ding, Q. Zhang, W. Yao, X. Xu, C.-Y. Lu, and J.-W. Pan, "Single quantum emitters in monolayer semiconductors," Nature Nanotech. **10**(6), 497–502 (2015).
11. M. Koperski, K. Nogajewski, A. Arora, V. Cherkez, P. Mallet, J.-Y. Veuillen, J. Marcus, P. Kossacki, and M. Potemski, "Single photon emitters in exfoliated WSe_2 structures," Nature Nanotech. **10**(6), 503–506 (2015).
12. C. Chakraborty, L. Kinnischtzke, K. M. Goodfellow, R. Beams, and A. N. Vamivakas, "Voltage-controlled quantum light from an atomically thin semiconductor," Nature Nanotech. **10**(6), 507–511 (2015).
13. A. Srivastava, M. Sidler, A. V. Allain, D. S. Lembke, A. Kis, and A. Imamoğlu, "Optically active quantum dots in monolayer WSe_2," Nature Nanotech. **10**(6), 491–496 (2015).
14. P. Tonndorf, R. Schmidt, R. Schneider, J. Kern, M. Buscema, G. A. Steele, A. Castellanos-Gomez, H. S. J. van der Zant, S. M. de Vasconcellos, and R. Bratschitsch, "Single-photon emission from localized excitons in an atomically thin semiconductor," Optica **2**(4), 347–352 (2015).
15. A. Branny, S. Kumar, R. Proux, B. D. Gerardot, "Deterministic strain-induced arrays of quantum emitters in a two-dimensional semiconductor," 1–10, http://arxiv.org/abs/1610.01406 (2016).
16. C. Palacios-Berraquero,D. M. Kara, A. R.-P. Montblanch, M. Barbone, P. Latawiec, D. Yoon, A. K. Ott, M. Loncar, A. C. Ferrari, M. Atature, "Large-scale quantum-emitter arrays in atomically thin semiconductors," http://arxiv.org/abs/1609.04427 (2016).
17. A. Castellanos-Gomez,M. Buscema,R. Molenaar,V. Singh, L. Janssen, J. S. J. van der Zant, G. Steele "Deterministic transfer of two-dimensional materials by all-dry viscoelastic stamping," 2D Materials, **1(1)**, 11002 (2014).
18. G. V. Astakhov, D. R. Yakovlev, V. P. Kochereshko,W. Ossau, W. Faschinger, J. Puls, A. Waag, "Binding energy of charged excitons in ZnSe-based quantum wells," Phys. Rev. B **65**(16), 165335 (2002).
19. F. Cadiz,C. Robert,G. Wang,W. Kong,X. Fan,M. Blei, … B. Urbaszek, "Ultralow power threshold for laser induced changes in optical properties of 2D Molybdenum dichalcogenides," 2D Materials, **3**(4), 1–16 (2016).
20. N. Lundt, E. Cherotchenko, O. Iff, X. Fan, Y. Shen, P. Bigenwald, A. Kavokin, S. Höfling, C. Schneider, "The interplay between excitons and trions in a monolayer of $MoSe_2$," arXiv:1702.04231 (2017).
21. Y. V. Morozov,M. Kuno, "SI - Optical constants and dynamic conductivities of single layer MoS_2, $MoSe_2$, and WSe_2," Applied Physics Letters, **1**(2015), 1689–1699 (2015).
22. C. Robert, D. Lagarde, F. Cadiz, G. Wang, B. Lassagne, T. Amand, A. Balocchi, P. Renucci, S. Tongay, B. Urbaszek, and X. Marie, "Exciton radiative lifetime in transition metal dichalcogenide monolayers," Physical Review B, **93**(20), 205423 (2016).
23. N. Kumar, Q. Cui, F. Ceballos, D. He, Y. Wang, H. Zhao, "Exciton-exciton annihilation in MoSe 2 monolayers," Phys. Rev. B **89(12)** 1–6 (2014).
24. Z. M. Ao,W. T. Zheng, Q. Jiang, "The effects of electronic field on the atomic structure of the graphene/-SiO(2) interface," Nanotechnology, **19**(27), 275710 (2008).
25. Y. K. Koh, D. G. Cahill, "Frequency dependence of the thermal conductivity of semiconductor alloys," Phys. Rev. B, **76**(7), 1–5 (2007).
26. Y.-M. He, S. Höfling, C. Schneider, "Phonon induced line broadening and population of the dark exciton in a deeply trapped localized emitter in monolayer WSe_2," Opt. Exp., **24**(8), 8066 (2016).
27. S. Tian, Z. Wei, Y. Li, H. Zhao, X. Fang, J. Tang, D. Fang, L. Sun, G. Liu, B. Yao, X. Ma "Surface state and optical property of sulfur passivated InP," Materials Science in Semiconductor Processing, **17**, 33–37 (2014).
28. C. E. J. Mitchell, I. G. Hill, A. B. McLean, Z. H. Lu, "Sulfur passivated InP(100): Surface gaps and electron counting," Applied Surface Science, **104–105**, 434–440 (1996).